 CMES, vol.38, no.1, pp.1-23, 2008

A Numerical Meshfree Technique for the Solution of the MEW Equation

Sirajul Haq[1], **Siraj-ul-Islam**[2] **and Arshed Ali**[3]

Abstract: In this paper we propose a meshfree technique for the numerical solution of the modified equal width wave (MEW) equation. Combination of collocation method using the radial basis functions (RBFs) with first order accurate forward difference approximation is employed for obtaining meshfree solution of the problem. Different types of RBFs are used for this purpose. Performance of the proposed method is successfully tested in terms of various error norms. In the case of non-availability of exact solution, performance of the new method is compared with the results obtained from the existing methods. Propagation of a solitary wave, interaction of two solitary waves, a train of solitary waves, conservative properties in terms of mass, momentum and energy are investigated. The elementary stability analysis of the method is discussed both theoretically and numerically.

Keywords: Generalized equal width wave (GEW) equation, Modified equal width wave (MEW) equation, Radial basis functions (RBFs), Solitary wave, Stability analysis.

1 Introduction

The regularized long wave equation (RLW) is an important nonlinear equation, which describes a large number of physical phenomena [Abdulloev, Bogolubsky and Makhankov (1976)] and [Peregrine (1966)] and has the following form,

$$U_t + U_x + \varepsilon U U_x - \mu U_{xxt} = 0, \tag{1.1}$$

[1] Faculty of Engineering Sciences, GIK Institute of Engineering Sciences & Technology Topi (NWFP), Pakistan. Email: siraj_jcs@yahoo.co.in

[2] Corresponding author. NWFP University of Engineering and Technology Peshawar, Phone # (92-91)921796-98 Ext: , Fax # (92-91) 9216663. University of Engineering & Technology Peshawar (NWFP), Pakistan. Email: siraj-ul-islam@nwfpuet.edu.pk

[3] Faculty of Engineering Sciences, GIK Institute of Engineering Sciences & Technology Topi (NWFP), Pakistan. Email: arshad_math@hotmail.com

where the parameters ε and μ are related to small amplitude and long-wavelength [see Siraj-ul-Islam, Sirajul Haq and Arshed Ali (2008)]. The subscripts t and x given in Eq. (1.1) represent differentiation with respect to t and x.

The EW equation derived by [Morrison, Meiss and Carey (1984)], is a special form of RLW equation (1.1) and is given by,

$$U_t + \varepsilon U U_x - \mu U_{xxt} = 0. \tag{1.2}$$

The EW equation (1.2) is a special case of generalized equal width wave (GEW) equation [Evans and Raslan (2005)], which is of the form,

$$U_t + \varepsilon U^m U_x - \mu U_{xxt} = 0, \tag{1.3}$$

where m is a positive integer.

The exact solitary wave solution of GEW equation (1.3) is obtained by [Hamdi, Enright, Schiesser and Gottlieb (2003)]. [Evans and Raslan (2005)] gave various solitary wave solutions of the GEW equation using a quadratic B-splines finite element method.

Another particular case of GEW equation (1.3) is known as modified equal width wave (MEW) equation, which has the form

$$U_t + \varepsilon U^2 U_x - \mu U_{xxt} = 0. \tag{1.4}$$

The MEW equation contains a cubic nonlinearity and exhibits pulse-like solitary wave having the same width with both positive and negative amplitudes [Wazwaz (2006)]. Several numerical methods have been introduced in the literature for the solution the MEW equation [Zaki (2000)], [Esen (2006)], [Wazwaz (2006)], [Saka (2007)] and [Esen and Kutluay (2008)].

In this paper, we develop a meshfree collocation method with different types of RBFs for the numerical solution of the MEW equation. Conservative properties of the MEW equation related to mass, momentum and energy are also investigated. The meshfree technique uses RBFs which are one of the primary tools for interpolating multi-dimensional data. This approach has been extensively used to find numerical solutions of various types of partial differential equations (PDEs). A key feature of the meshfree method is its ability to handle arbitrary scattered data, and its extension to several space dimensions. Moreover, it avoids mesh-generation, which is the major problem in the finite-difference, finite element and spectral methods. [Kansa (1990)] has pioneered this technique by applying RBFs, particularly the multiquadric (MQ), to a scattered data with applications to computational fluid-dynamics, which was modified by [Fasshauer (1996)] to the Hermite

type collocation method for the invertibility of the collocation matrix. Convergence order estimates of meshfree collocation methods using radial basis functions are discussed by [Franke and Schaback (1998)]. Due to simple applicability, Kansa's method is recently extended to solve various types ordinary and partial differential equations including [Franke and Schaback (1998)], heat transfer [Hon and Mao (1998)], shallow water equation for tide and current simulations [Hon, Cheung, Mao and Kansa (1999)], the free boundary-value problems [Wu and Hon (2003)], 1-D nonlinear Burgers' equation with the shock wave [Li, Chen and Pepper (2003)], transport equation [Lorentz, Narcowich and Ward (2003)], MLPG "Mixed" Approach [Atluri, Han, Rajendran (2004)], a class of KdV equations [Khattak and Siraj-ul-Islam (2007)], RLW equation [Siraj-ul-Islam, Sirajul Haq and Arshed Ali (2008)], a system of nonlinear PDEs [Siraj-ul-Islam, Sirajul Haq and Marjan Uddin (2008)], Lid-driven cavity flow problem [Chantasiriwan (2006)] and recently, Darcy flow [Kosec and Sarler (2008)] and see the references therein.

The rest of the paper is organized as follows. In Section 2, we develop algorithm for the numerical solution of the MEW equation. Section 3, is devoted to stability analysis of the method. In Section 4, we present numerical analysis related to different types of the MEW equations. In Section 5, we summarize the results.

2 Construction of the proposed method

We consider the MEW equation (1.4) subject to the Dirichlet boundary conditions,

$$U(a,t) = \alpha_1(t), \quad U(b,t) = \alpha_2(t) \tag{2.1}$$

and initial condition,

$$U(x,0) = f(x), \quad x \in [a,\, b] \subset R. \tag{2.2}$$

where $f(x)$ is a localized disturbance inside the interval $[a,b]$ and $U \to 0$ as $x \to \pm\infty$. The time derivative present in the MEW equation is approximated by a first order accurate forward difference formula and the spatial derivative are approximated by a suitable RBF after applying the $\theta-$weighted, $(0 \le \theta \le 1)$ scheme at two successive time levels n and $n+1$ like given below:

$$\frac{\left(U^{(n+1)} - U^{(n)}\right)}{\Delta t} + \theta\left(\varepsilon(U^2)^{(n+1)}U_x^{(n+1)}\right) + (1-\theta)\left(\varepsilon(U^2)^{(n)}U_x^{(n)}\right) - \mu\frac{\left(U_{xx}^{(n+1)} - U_{xx}^{(n)}\right)}{\Delta t} = 0 \tag{2.3}$$

where $U^{(n)} = U(x,t^{(n)})$, $t^{(n)} = t^{(n-1)} + \Delta t$ and Δt is time step size.

Eq. (2.3) is linearised by approximating the nonlinear term $(U^2)^{(n+1)}U_x^{(n+1)}$, using the following formula [Rubin and Graves (1975)]:

$$(U^2)^{(n+1)}U_x^{(n+1)} \approx (U^{(n)})^2 U_x^{(n+1)} + 2U^{(n)}U_x^{(n)}U^{(n+1)} - 2(U^{(n)})^2 U_x^{(n)} \tag{2.4}$$

From Eqs. (2.3) and (2.4) we obtain

$$U^{(n+1)} + \Delta t\theta\left[\varepsilon\left\{(U^{(n)})^2 U_x^{(n+1)} + 2U^{(n)}U_x^{(n)}U^{(n+1)}\right\}\right] - \mu U_{xx}^{(n+1)} = U^{(n)} + \Delta t\left[\varepsilon(3\theta-1)(U^{(n)})^2 U_x^{(n)}\right] - \mu U_{xx}^{(n)}. \tag{2.5}$$

Let $x_i,\ i = 1, 2, ..., N$ be the collocation points in the interval $[a,\ b]$ such that $x_1 = a$ and $x_N = b$. The solution of Eq. (1.4) can be approximated by

$$U^{(n)}(x) = \sum_{j=1}^{N} \lambda_j^{(n)} \psi(r_j), \tag{2.6}$$

where ψ is a radial basis function and $r_j(x) = \sqrt{(x-x_j)^2}$ represents the Euclidean distance between x and x_j, where x_j's are known as centers. The unknown parameters λ_j in Eq. (2.6) are to be determined by the collocation method. Therefore for each collocation point x_i, Eq. (2.6) can be written as

$$U^{(n)}(x_i) = \sum_{j=1}^{N} \lambda_j^{(n)} \psi(r_{ij}), \quad i = 1, 2, ..., N, \tag{2.7}$$

where $r_{ij} = \sqrt{(x_i - x_j)^2}$.
Eq. (2.7) can be expressed in a matrix form as

$$U^{(n)} = A\lambda^{(n)}, \tag{2.8}$$

where $A = [\psi(r_{ij}) : 1 \le i \le N,\ 1 \le j \le N\ ]$ and $\lambda^{(n)} = [\lambda_1^{(n)}, \lambda_2^{(n)}, ..., \lambda_N^{(n)}]^T$.
The matrix A can be split into two matrices A_d and A_b corresponding to $N-2$ interior points and two boundary points in the following form:

$$A = A_d + A_b, \tag{2.9}$$

where $A_d = [\psi(r_{ij}) :\ 2 \le i \le N-1,\ 1 \le j \le N$ and 0 elsewhere],

$A_b = [\psi(r_{ij}) :\ i = 1, N,\ 1 \le j \le N$ and 0 elsewhere].

The following radial basis functions will be used for numerical approximation of the problem:

Multiquadric (MQ) $\psi(r_j) = \sqrt{r_j^2 + c^2}$

Gaussian (GA) $\psi(r_j) = e^{-c\, r_j^2}$

Thin Plate Spline (TPS) $\psi(r_j) = r_j^{2m} \log(r_j)$, where $m = 2$ in our case.

The constant c is known as the shape parameter of the radial basis functions and its value is a key factor for accuracy of the solution. Optimal value of c is to be found numerically for each radial basis function and for each problem separately.

Using Eq. (2.8) in Eqs. (2.5) and (2.1), we get the following matrix form:

$$\left[A - \mu C + \theta \Delta t \left\{ \varepsilon \left(\left(U^{(n)}\right)^2 * B + 2 \left(U^{(n)} \circ U_x^{(n)} \right) * A_d \right) \right\} \right] \lambda^{(n+1)} = \left[A - \mu C + \Delta t \left\{ \varepsilon (3\theta - 1) \left(U^{(n)}\right)^2 * B \right\} \right] \lambda^{(n)} + E^{(n+1)}, \quad (2.10)$$

where B and C are $N \times N$ matrices such that

$$B = \left[\psi'(r_{ij}) : 2 \le i \le N-1,\ 1 \le j \le N \text{ and 0 elsewhere} \right],$$

$$C = \left[\psi''(r_{ij}) : 2 \le i \le N-1,\ 1 \le j \le N \text{ and 0 elsewhere} \right],$$

$$\psi'(r_{ij}) = \frac{d}{dx} \psi \left(\sqrt{(x - x_j)^2} \right) |_{x = x_i},$$

$$\psi''(r_{ij}) = \frac{d^2}{dx^2} \psi \left(\sqrt{(x - x_j)^2} \right) |_{x = x_i},$$

$U_x^{(n)} = B\lambda^{(n)}$ and $E^{(n+1)} = [\alpha_1(t^{(n+1)}),\ 0,\ 0, ...,\ 0,\ \alpha_2(t^{(n+1)})]^T$.

The symbol '*' means that the ith component of the vector $U^{(n)}$ is multiplied to every element of the ith row of the matrix B and the symbol '$\circ$' means that ith component of the vector $U^{(n)}$ is multiplied to ith component of vector $U_x^{(n)}$. Eq. (2.10) can be rewritten as

$$\lambda^{(n+1)} = M^{-1} N \lambda^{(n)} + M^{-1} E^{(n+1)}, \quad (2.11)$$

where $M = \left[A - \mu C + \theta \Delta t \left\{ \varepsilon \left(\left(U^{(n)}\right)^2 * B + 2 \left(U^{(n)} \circ U_x^{(n)} \right) * A_d \right) \right\} \right]$ and

$$N = \left[A - \mu C + \Delta t \left\{ \varepsilon (3\theta - 1) \left(U^{(n)}\right)^2 * B \right\} \right].$$

From Eqs. (2.11) and (2.8), we can write

$$U^{(n+1)} = A M^{-1} N A^{-1} U^{(n)} + A M^{-1} E^{(n+1)}. \quad (2.12)$$

[Hon and Schaback (2001)] have shown that the non-singularity of the matrix M can not be proved in general, therefore, it is not possible to show that the scheme is well-posed in all such cases. However, singularities in practical problems are rare.

Eq. (2.10) represents a system of N linear equations in N unknown parameters λ_j. This system can be solved by the Gaussian elimination method. The collocation matrix corresponding to the TPS becomes highly ill-conditioned because of a singularity at r_{ii} where the sets of centers and collocation points coincide. This problem does not occur in rest of the two RBFs. However, in the case of TPS we use the limiting value $\lim_{r\to 0} r^4 \log(r) = 0$, to obtain a solvable system. In this case, the Gauss elimination method with partial pivoting is used to solve the system of linear equations. The approximate solution can be found from Eq. (2.6) at any point in the interval $[a, b]$ after finding the values of the unknown parameters $\lambda_j,\ j = 1,2,...,N$ at each time level. The results of this section can be summarized in the following algorithm.

2.1 Algorithm

The algorithm works in the following manner:

1. Choose N collocation points from the domain set $[a, b]$.
2. Choose the parameters Δt and θ such that $(0 \leq \theta \leq 1)$.
3. Calculate the initial solution $U^{(0)}$ from Eq. (2.2) and then use Eq. (2.8) to find $\lambda^{(n)} = A^{-1}U^{(n)}$.
4. The parameters $\lambda_j^{(n+1)}$ are calculated from Eq. (2.10).
5. The approximate solution $U^{(n+1)}$at the successive time levels is obtained from step 4 and Eq. (2.8)

3 Stability Analysis

In this section, we present the stability of the RBF approximation (2.10) using the matrix method. Eq. (1.4) can be linearized by assuming the quantity U^2 in the nonlinear term U^2U_x as locally constant. The error $e^{(n)}$ at the n*th* time level is given by

$$e^{(n)} = U_{exact}^{(n)} - U_{app}^{(n)}, \tag{3.1}$$

where $U_{exact}^{(n)}$, $U_{app}^{(n)}$ are the exact and the numerical solutions at the n*th* time level. The error equation for the linearized MEW equation can be written as;

$$[R + \theta\Delta tS]e^{(n+1)} = [R - \Delta t(1-\theta)S]e^{(n)}, \tag{3.2}$$

where $R = [A - \mu C]A^{-1}$ and $S = \varepsilon \left(\left(U^{(n)} \right)^2 * B \right) A^{-1}$.

Eq. (3.2) can be rewritten as

$$e^{(n+1)} = Te^{(n)}. \tag{3.3}$$

where $T = [I + \theta \Delta t H]^{-1}[I - \Delta t(1-\theta)H]$ and $H = R^{-1}S$. The numerical scheme is stable if $\| T \|_2 \leq 1$, which is equivalent to $\rho(T) \leq 1$, where $\rho(T)$ denotes the spectral radius of the matrix T. From the definition of the matrix T in Eq. (3.3), the stability is satisfied automatically in the following manner

$$\left| \frac{1 - \Delta t(1-\theta)\lambda_H}{1 + \Delta t \theta \lambda_H} \right| \leq 1, \tag{3.4}$$

where $\lambda_H \geq 0$ is the eigenvalues of the matrix H. This fact is also verified from Tab. 3(a) and Figure 2, where minimum eigenvalues are calculated versus different values of shape parameter c.

When $\theta = 0.5$, the inequality (3.4) becomes

$$\left| \frac{1 - 0.5\Delta t \lambda_H}{1 + 0.5\Delta t \lambda_H} \right| \leq 1. \tag{3.5}$$

For $\theta = 0$, the inequality (3.4) becomes

$$|1 - \Delta t \lambda_H| \leq 1, \tag{3.6}$$

i.e., $\Delta t \leq \frac{2}{\lambda_H}$ and $\lambda_H \geq 0$. Thus for $\theta = 0$, the scheme is conditionally stable.

The stability of the scheme (2.10) also depends on the condition number of the matrix T, the weight parameter θ, the minimum distance between any two collocation points h in the domain set $[a,\ b]$, and the local shape parameter c. [Cheng, Golberg, Kansa and Zammito (2003)] showed that when c is very large then the RBFs system convergence is of exponential order but the solution breaks down when c is greater than the limiting value. The condition number of the matrix T versus different values of the shape parameter c is shown in Tab. 3(b) and Figure 3 corresponding to problem 4.1 for MQ case only. In Figure 4, we have plotted error for different values of the shape parameter c. Critical values of the shape parameter c in this case are 0.1 and 1.1 and the condition numbers of the matrix T corresponding to these values are given by 1.0037×10^0 and 5.5482×10^{14} respectively. It is clear from Figures 2-4 and Tabs. 3(a)-3(b), that if the value of the shape parameter c is chosen below or beyond the critical values, then the solution breaks down and hence the method becomes unstable. The interval of stability for the shape parameter c in this case is (0.1, 1.1). In case of the parameter free RBFs such as TPS, the stability and conditioning depend on the weight parameter θ, eigenvalue λ_H.

4 Numerical Tests and Results

In this section we present the results obtained from the meshfree method (2.10) proposed for the numerical solution of the MEW Eqs. (1.4) and (2.1)-(2.2) for a single solitary wave, an interaction of two solitary waves and a train of solitary waves generated from Maxwellian initial condition. The solution produced by the new method preserve mass, momentum and energy of the waves during propagation. The accuracy of the scheme is measured by using the following error norms:

$$L_2 = \|U_{exact} - U_{app}\|_2 = \sqrt{h \sum_{j=0}^{N} \left|(U_{exact})_j - (U_{app})_j\right|^2},$$

and

$$L_\infty = \|U_{exact} - U_{app}\|_\infty = \max_j \left|(U_{exact})_j - (U_{app})_j\right|,$$

where U_{exact}, U_{app} represent the exact and approximate solutions respectively and h (the minimum distance between any two collocation points of the domain set $[a, b]$). The value of the weight parameter θ used in the main scheme (2.10) is taken as 0.5 for each problem.

The MEW equation possesses three conservation properties related to mass, momentum and energy given by [Evans and Raslan (2005)] in the following manners respectively:

$$C_1 = \int_a^b U\,dx \approx h \sum_{i=1}^{N} U(x_i),$$

$$C_2 = \int_a^b \left(U^2 + \mu\,(U_x)^2\right) dx \approx h \sum_{i=1}^{N} \left[(U(x_i))^2 + \mu\,(U_x(x_i))^2\right],$$

$$C_3 = \int_a^b U^4\,dx \approx h \sum_{i=1}^{N} (U(x_i))^4.$$

4.1 Propagation of Single Solitary Wave

The following analytical solution of Eq. (1.4) is given in [Zaki (2000)],

$$U(x,t) = A\,sech\left[k\,(x - x_o - pt)\right]. \tag{4.1}$$

This equation represents a single solitary wave of amplitude $A = \sqrt{6p/\varepsilon}$, where p is the velocity of the wave and $k = \sqrt{1/\mu}$. The initial condition of Eq. (1.4) is given by

$$U(x,0) = Asech[k(x-x_o)]. \tag{4.2}$$

The boundary conditions are extracted form the exact solution (4.1). We choose the parameters values $A = 0.25$, $x_o = 30$, $\varepsilon = 3$, $\mu = 1$, the number of collocation points $N = 800$ and time steps $\Delta t = 0.2$ and 0.05 and the space interval $0 \leq x \leq 80$ in order to compare our results with those given in [Esen and Kutluay (2008)] and [Evans and Raslan (2005)]. The numerical tests are performed using the three RBFs MQ, GA and TPS. The simulation is done up to time $t = 20$. The error norms L_∞, L_2 and conservation quantities C_1, C_2 and C_3 are computed, which are shown in the Tabs. 1(a)-1(b) along with the results of the previous methods [Esen and Kutluay (2008)] and [Evans and Raslan (2005)] for comparison. From the numerical results given in Tab. 1(a) it is observed that throughout the simulation, the error norms L_∞ remains less than 1.008×10^{-6} and L_2 remains less than 1.61×10^{-6} for each of MQ and GA, while the upper bound for these error norms in the case of TPS are 5.414×10^{-6} and 6.269×10^{-6} respectively, for $\Delta t = 0.2$. Single solitary wave solutions at initial and different time levels are shown in Figure 1. During simulation it is observed form Tab. 1(a) that the error in the invariant quantities C_1, C_2 and C_3 approaches zero for both MQ and GA, however for TPS the error in the C_1 quantity approaches zero and maximum absolute error in the invariant quantities C_2 and C_3 remains less than 2.0×10^{-6} and 1.0×10^{-7} respectively. It can also be observed Tab. 1(b) that throughout the simulation, the upper bounds for the error norms L_∞, L_2 are 6.7×10^{-8} and 1.14×10^{-7} for MQ and GA respectively, while the maximum values of these error norms for TPS are 5.284×10^{-6} and 5.451×10^{-6} for $\Delta t = 0.05$.

In Tabs. 1(c), we have taken different values of $A = 0.25$, 0.5, 0.75 and 1.0 and keeping other parameters same in order to compare our results with those given in [Esen and Kutluay (2008)]. The algorithm is examined for $A = 0.25$, 0.5, 0.75 and 1.0 and the simulation is done up to $t = 20$ for each MQ, GA and TPS. The error norms L_∞, L_2 and conservation quantities C_1, C_2 and C_3 are computed, which are shown in the Tab. 1(c) along with the results of the previous methods [Esen and Kutluay (2008)] for comparison. It is clear from Tab. 1(c) that the error norms L_∞ and L_2 are small enough and the numerical values are in close proximity of the exact values during the run time of the proposed algorithm for each of the RBFs. It is also clear from Tab. 1(c) that the accuracy in terms of error norms L_∞ and L_2 increases as A decreases. For example, at $t = 20$ the error norms are $L_\infty = 4.61685 \times 10^{-5}$ and $L_2 = 6.97953 \times 10^{-5}$ for $A = 1$, whereas these are

Table 1(a): Comparisons of invariants and error norms for the single solitary wave with results from [Esen and Kutluay (2008)] and [Evans and Raslan (2005)], $A = 0.25$, $N = 800$, $\Delta t = 0.2$, $0 \leq x \leq 80$.

Method	Time	$L_\infty \times 10^4$	$L_2 \times 10^4$	C_1	C_2	C_3
MQ	0	0.0	0.0	0.785398	0.166667	0.0052083
	5	0.00244	0.00403	0.785398	0.166667	0.0052083
	10	0.00494	0.00806	0.785398	0.166667	0.0052083
	15	0.00748	0.01208	0.785398	0.166667	0.0052083
	20	0.01008	0.01610	0.785398	0.166667	0.0052083
GA	0	0.0	0.0	0.785398	0.166667	0.0052083
	5	0.00244	0.00403	0.785398	0.166667	0.0052083
	10	0.00494	0.00806	0.785398	0.166667	0.0052083
	15	0.00748	0.01208	0.785398	0.166667	0.0052083
	20	0.01008	0.01610	0.785398	0.166667	0.0052083
TPS	0	0.0	0.0	0.785398	0.166667	0.0052083
	5	0.03955	0.03605	0.785398	0.166665	0.0052082
	10	0.04375	0.04283	0.785398	0.166665	0.0052082
	15	0.04905	0.05213	0.785398	0.166665	0.0052082
	20	0.05414	0.06269	0.785398	0.166665	0.0052082
[Esen (2008)]	20	2.57638	2.70165	0.785398	0.166474	0.0052083
[Evans (2005)]	20	1.56954	2.02148	0.785286	0.166582	0.0052061

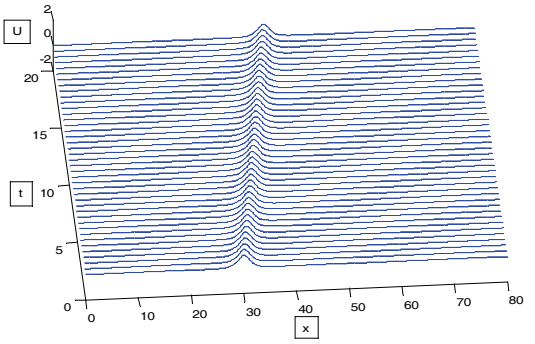

Fig. 1: Single solitary wave solutions, $N = 800$, $\Delta t = 0.2$

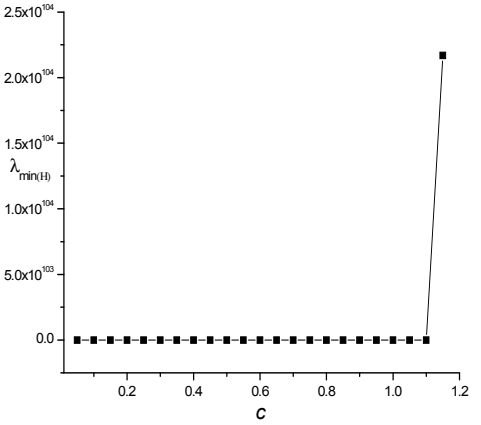

Fig. 2: Minimum eigenvalue of matrix H versus shape parameter *c*

$L_\infty = 2.5 \times 10^{-9}$ and $L_2 = 4.0 \times 10^{-9}$ for A = 0.25. The most accurate results are obtained when the values of the shape parameter $c = 0.9$ and 6.5 are used for the MQ and GA respectively. From the numerical given in Tabs. 1(a)-1(c), it is clear that the performance of the proposed meshfree method is better than the existing methods [Esen and Kutluay (2008)] and [Evans and Raslan (2005)].

The pointwise rates of convergence in space and time are calculated by using the following formulae:

$$\frac{\log_{10}\left(\|U_{exact} - U_{h_i}\| / \left\|U_{exact} - U_{h_{i+1}}\right\|\right)}{\log_{10}(h_i/h_{i+1})}$$

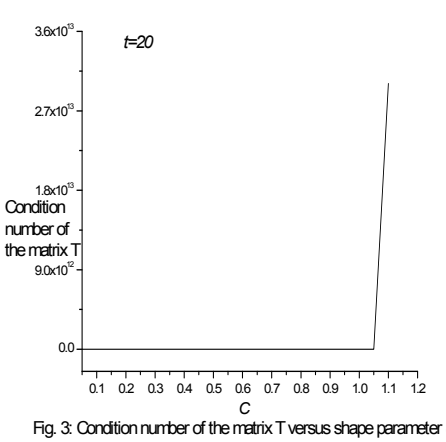

Fig. 3: Condition number of the matrix T versus shape parameter *c*

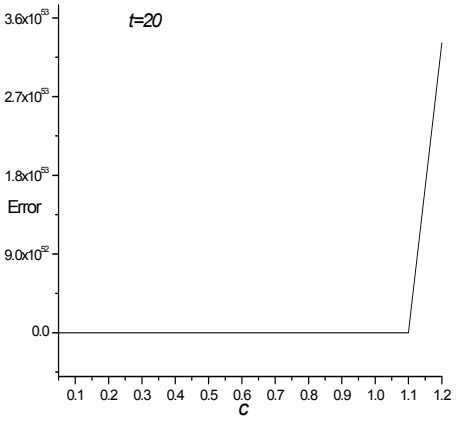

Fig. 4: Error versus shape parameter *c*

Table 1(b): Comparisons of invariants and error norms for the single solitary wave with results from [Esen and Kutluay (2008)] and [Evans and Raslan (2005)], $A = 0.25$, $N = 800$, $\Delta t = 0.05$, $0 \leq x \leq 80$.

Method	Time	$L_\infty \times 10^4$	$L_2 \times 10^4$	C_1	C_2	C_3
MQ	0	0.0	0.0	0.785398	0.166667	0.0052083
	10	0.00031	0.00050	0.785398	0.166667	0.0052083
	20	0.00063	0.00101	0.785398	0.166667	0.0052083
GA	10	0.00031	0.00050	0.785398	0.166667	0.0052083
	20	0.00067	0.00114	0.785398	0.166667	0.0052083
TPS	10	0.04364	0.04003	0.785398	0.166665	0.0052082
	20	0.05284	0.05451	0.785398	0.166665	0.0052082
[Esen (2008)]	20	2.56997	2.69281	0.785398	0.166474	0.0052083
[Evans (2005)]	20	2.49892	2.90517	0.784954	0.166476	0.0051995

and

$$\frac{\log_{10}\left(\|U_{exact} - U_{h_i}\| / \|U_{exact} - U_{h_{i+1}}\|\right)}{\log_{10}(\Delta t_i / \Delta t_{i+1})}.$$

The term U_{exact} is the exact solution, whereas U_{h_i} and $U_{\Delta t_i}$ are the numerical solutions with spatial step size and time step size Δt_i respectively. Computations are carried out with the different spatial and time step sizes to examine the point rates of convergence in space and time for each of the MQ, GA and TPS. In Tab. 2(a), the time step is kept fixed at $\Delta t = 0.05$ and the number of collocation points $N =$ 100, 200, 400, 600, 800 is varied to calculate the spatial rate of convergence for each of the RBFs approximations. It can be concluded from the Tab. 2(a) that

Table 1(c): Invariants and error norms for the single solitary wave, $\Delta t = 0.01$, $N = 800$, $0 \leq x \leq 80$.

	Time	$L_\infty \times 10^4$	$L_2 \times 10^4$	C_1	C_2	C_3
$A = 0.25$	0	0.0	0.0	0.785398	0.166667	0.0052083
MQ	20	0.000025	0.000040	0.785398	0.166667	0.0052083
GA	20	0.000025	0.000040	0.785398	0.166667	0.0052083
TPS	20	0.052774	0.054110	0.785398	0.166665	0.0052082
[Esen (2008)]	20	2.569562	2.692249	–	–	–
$A = 0.5$	0	0.0	0.0	1.570796	0.666667	0.0833333
MQ	20	0.003404	0.005176	1.570796	0.666667	0.0833333
GA	20	0.003340	0.005176	1.570796	0.666667	0.0833333
TPS	20	0.003340	0.005176	1.570796	0.666667	0.0833333
[Esen (2008)]	20	14.57568	18.26059	–	–	–
$A = 0.75$	0	0.0	0.0	2.356194	1.500000	0.4218750
MQ	20	0.057780	0.091244	2.356194	1.500000	0.4218750
GA	20	0.057780	0.091244	2.356194	1.500000	0.4218750
TPS	20	0.592772	0.825156	2.356194	1.499983	0.4218656
[Esen (2008)]	20	30.91793	43.95711	–	–	–
$A = 1.0$	0	0.0	0.0	3.141593	2.666667	1.3333333
MQ	20	0.461685	0.697953	3.141593	2.666666	1.3333333
GA	20	0.436168	0.697981	3.141594	2.666666	1.3333331
TPS	20	1.502736	2.253715	3.141592	2.666637	1.3333035
[Esen (2008)]	20	56.82131	82.85314	–	–	–

the convergence rate decreases with the smaller spatial step size. Both the error norms L_∞ and L_2 decreases slightly by increasing the number of collocation points N for each case of the given RBFs. In the Tab. 2(b), the number of the collocation points is kept fixed at $N = 800$ and the time step size $\Delta t_i = 1,\ 0.5,\ 0.2,\ 0.1, 0.05$ is varied to compute the time rate of convergence for each of the RBFs approximation. It can be noted from the Tab. 2(b), that the rate of convergence increases with the smaller time step size for MQ and GA, while the rate of convergence decreases for TPS.

4.2 Interaction of two solitary waves

Interaction of the two positive solitary waves is studied by using the initial condition

$$U(x,0) = A_1 \sec h\left[k(x-x_1)\right] + A_2 \sec h\left[k(x-x_2)\right], \tag{4.3}$$

where $k = \sqrt{1/\mu}$.

Table 2(a): Space rate of convergence at $t = 20$, $\Delta t = 0.05$, $A = 0.25$, $0 \leq x \leq 80$.

MQ	N	$L_\infty \times 10^5$	Order	$L_2 \times 10^5$	Order
	100	106.34388	—	136.55155	—
	200	0.09462	10.13427	0.09984	10.41747
	400	0.00626	3.91686	0.01006	3.31092
	600	0.00630	-0.01307	0.01006	0.00000
	800	0.00630	0.00061	0.01006	0.00000
GA					
	100	106.28949	—	136.35656	—
	200	0.08786	10.24054	0.09275	10.52181
	400	0.00626	3.80986	0.01006	3.20451
	600	0.00630	-0.01307	0.01006	0.00000
	800	0.00630	0.00061	0.01006	0.00000
TPS					
	100	430.00635	—	519.66539	—
	200	39.62500	3.43988	41.67800	3.64022
	400	4.38030	3.17731	4.50080	3.21103
	600	1.24020	3.09300	1.28910	3.06472
	800	0.52836	2.99198	0.54506	3.01847

We choose the parameters $\alpha_1 = 0$, $\alpha_2 = 0$, $A_1 = 1$, $A_2 = 0.5$, $\mu = 1$, $\varepsilon = 3$, $x_1 = 15$, $x_2 = 30$ and the space interval $0 \leq x \leq 80$ to compare our results with those in the literature [Esen and Kutluay (2008)]. The initial condition (4.3) with these parameters gives solitary waves with the amplitudes 1 and 0.5 occurring at $x = 15$ and $x = 30$ respectively. Computations are carried out up to time $t = 80$, time step $\Delta t = 0.2$ and the number of collocation points $N = 800$. In the process of interaction, the larger and the smaller waves interact and separate while preserving their original shapes and velocities. Shapes of both the waves during the interaction at time $t = 30,\ 35,\ 40$ and after interaction at time $t = 55$ and 80 are shown in Figures 5-10 for each case of the RBFs. At $t = 80$, the smaller solitary wave with the amplitude 0.49878 and peak position located at $x = 37.7$, larger solitary wave with the amplitude 0.99931 and peak position located at $x = 56.8$ are obtained. It is found that the absolute difference between amplitudes of the larger solitary wave at $t = 0$ and $t = 80$ is $6.9 \times 10^{-4}$and that for the smaller wave is 1.22×10^{-3} for each MQ, GA and TPS. The invariant quantities C_1, C_2 and C_3 at various times are documented in the Tabs. 4-5 for MQ, GA and TPS. During simulation it is observed that the upper bounds for the maximum absolute errors of the invariant quantities C_1, C_2 and C_3 remain less than 1.0×10^{-6}, 4.0×10^{-3} and 4.0×10^{-3}

Table 2(b): Time rate of convergence at $t = 20$, $N = 800$, $A = 0.25$, $0 \leq x \leq 80$.

MQ	Δt_i	$L_\infty \times 10^5$	Order	$L_2 \times 10^5$	Order
	1	2.51860	—	4.02510	—
	0.5	0.62978	1.99970	1.00630	1.99996
	0.2	0.10076	2.00005	0.16099	2.00012
	0.1	0.02519	2.00006	0.04024	2.00012
	0.05	0.00630	2.00003	0.01006	2.00000
GA					
	1	2.51860	—	4.02510	—
	0.5	0.62978	1.99970	1.00630	1.99996
	0.2	0.10076	2.00005	0.16099	2.00012
	0.1	0.02519	2.00006	0.04024	2.00012
	0.05	0.00630	2.00003	0.01006	2.00000
TPS					
	1	2.48890	—	4.28330	—
	0.5	0.93173	1.41752	1.33170	1.68545
	0.2	0.54140	0.59248	0.62692	0.82222
	0.1	0.53089	0.02828	0.55902	0.16538
	0.05	0.52836	0.00689	0.54506	0.03648

Table 3(a): Minimum eigenvalues of the matrix H versus shape parameter c at $t = 20$, $N = 800, A = 0.25, \Delta t = 0.2, 0 \leq x \leq 80$.

c	$\lambda_{\min(H)}$	$L_\infty-$error	L_2-error
0.10	4.0727E-28	1.5082 E-03	1.7779 E-03
0.20	1.7745 E-30	4.8175 E-06	6.1960 E-06
0.30	2.9156 E-28	1.0135 E-06	1.6188 E-06
0.40	4.0920 E-26	1.0076 E-06	1.6099 E-06
0.50	3.8133 E-22	1.0076 E-06	1.6099 E-06
0.60	-3.3065 E-19	1.0076 E-06	1.6099 E-06
0.70	-1.9630 E-14	1.0076 E-06	1.6099 E-06
0.80	-1.2648 E-12	1.0076 E-06	1.6099 E-06
0.90	1.4355 E-11	1.0076 E-06	1.6099 E-06
0.95	8.5037 E-06	1.0076 E-06	1.6099 E-06
1.00	-4.9828 E-04	1.0076 E-06	1.6099 E-06
1.10	1.1138 E-06	1.0076 E-06	1.6099 E-06
1.15	2.1696 E104	1.5232 E+54	3.0458 E+53

Table 3(b): Condition number versus shape parameter c at $t = 20$, $N = 800$, $\Delta t = 0.2$, $A = 0.25$, $0 \leq x \leq 80$.

c	Condition number of the matrix T	$L_\infty-$error	c	Condition number of the matrix T	$L_\infty-$error
0.10	1.0037 E00	1.5082 E-03	0.70	8.5042 E08	1.0076 E-06
0.20	1.0038 E00	4.8175 E-06	0.80	1.6792 E13	1.0076 E-06
0.30	1.0038 E00	1.0135 E-06	0.90	7.5709 E11	1.0076 E-06
0.40	1.0044 E00	1.0076 E-06	1.00	1.1586 E14	1.0076 E-06
0.50	1.2797 E00	1.0076 E-06	1.10	5.5482 E14	1.0076 E-06
0.60	2.9853 E03	1.0076 E-06	1.20	9.2212 E25	7.6486 E+58

respectively, for each MQ, GA and TPS. The values of shape parameter for the parameter dependent RBFs MQ and GA are $c = 0.9$ and 6.5 respectively.

Table 4: Invariant quantities for interaction of two solitary waves

Our method (MQ)				[Esen (2008)]		
Time	C_1	C_2	C_3	C_1	C_2	C_3
0	4.712388	3.333336	1.416670	4.712388	3.329462	1.416669
20	4.712389	3.332190	1.415525	4.712387	3.328361	1.415523
40	4.712389	3.330941	1.414054	4.712385	3.327112	1.414050
55	4.712389	3.330700	1.414073	4.712386	3.326393	1.414062
60	4.712389	3.330416	1.413787	4.712388	3.326228	1.413785
80	4.712389	3.330236	1.412675	4.712389	3.325434	1.412671

Table 5: Invariant quantities for interaction of two solitary waves.

Our method (GA)				Our method (TPS)		
Time	C_1	C_2	C_3	C_1	C_2	C_3
0	4.712388	3.333336	1.416670	4.712388	3.333336	1.416670
20	4.712389	3.332190	1.415525	4.712389	3.332190	1.415525
40	4.712389	3.330941	1.414054	4.712389	3.330941	1.414054
55	4.712389	3.330700	1.414073	4.712389	3.330700	1.414073
60	4.712389	3.330416	1.413787	4.712389	3.330416	1.413787
80	4.712389	3.330236	1.412675	4.712389	3.330236	1.412675

4.3 The Maxwellian initial condition

The third numerical experiment of the proposed scheme is concerned with the generation of a number of solitary waves from Maxwellian initial condition. The Maxwellian initial condition is given by

$$U(x,0) = \exp(-x^2). \tag{4.4}$$

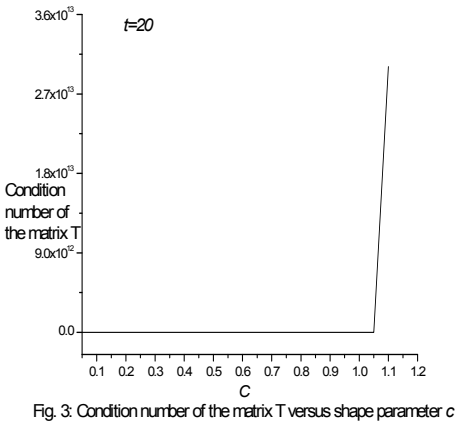

Fig. 3: Condition number of the matrix T versus shape parameter *c*

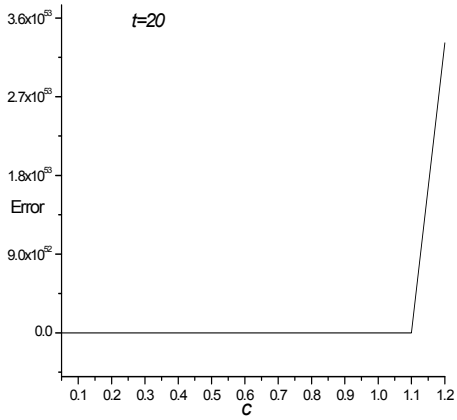

Fig. 4: Error versus shape parameter *c*

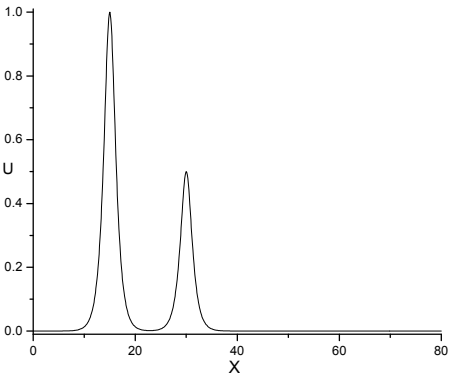

Fig. 5: Interaction of solitary waves at *t=0*

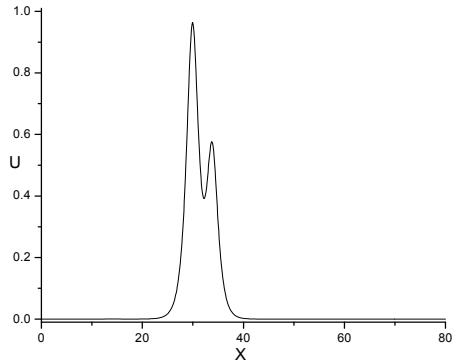

Fig. 6: Interaction of solitary waves at *t=30*

The generation of a number of solitary waves from Maxwell initial condition (4.4) depends on the value of μ. By reducing the value of μ, more solitary waves can be obtained [see Zaki (2000)] i.e. for $\mu >> \mu_c$, where μ_c is some critical value,

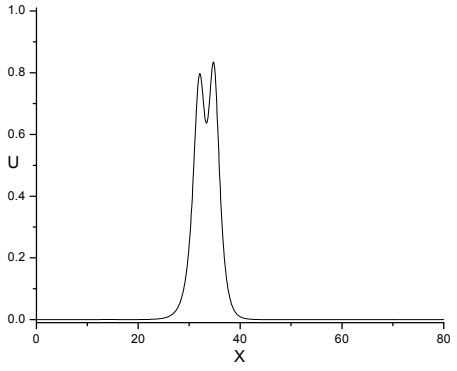

Fig. 7: Interaction of solitary waves at *t=35*

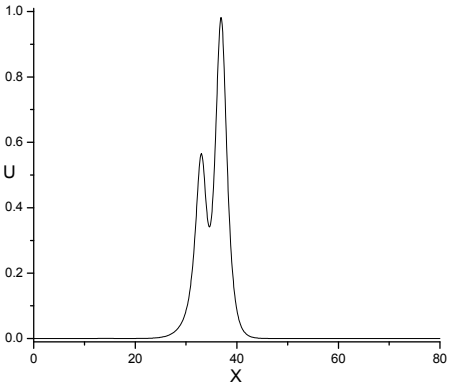

Fig. 8: Interaction of solitary waves at *t=40*

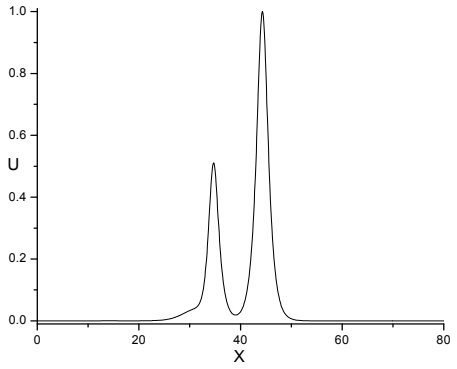

Fig. 9: Interaction of solitary waves at *t=55*

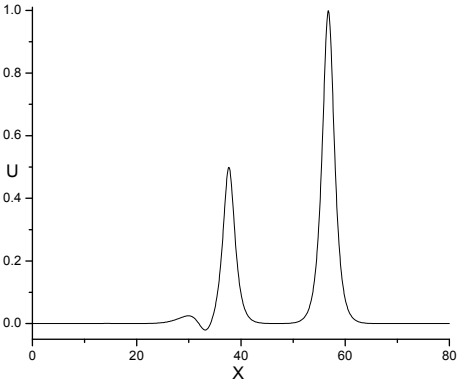

Fig. 10: Interaction of solitary waves at *t=80*

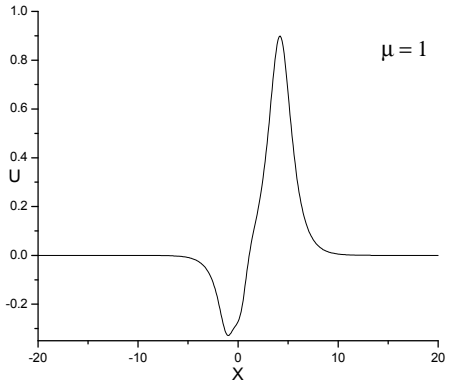

Fig. 11: Solitry waves from Maxwellian condition, *t=12*

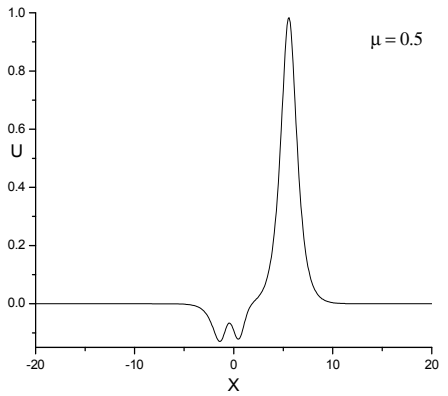

Fig. 12: Solitary waves from Maxwellian condition, *t=12*

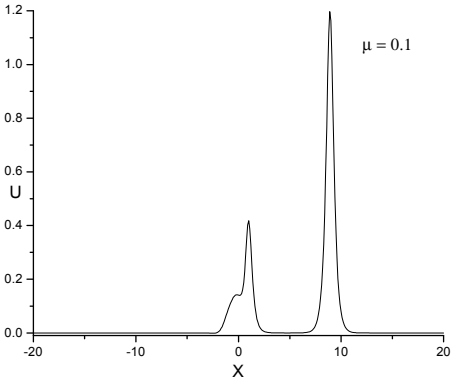

Fig. 13: Solitary waves from Maxwellian codition, *t=12*

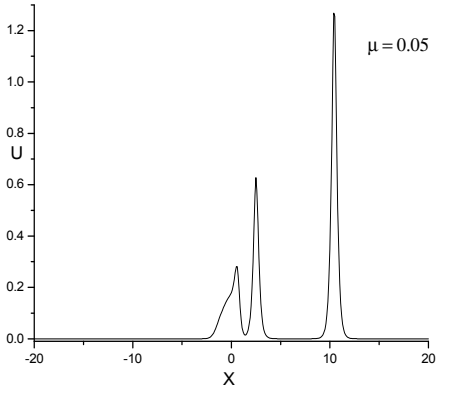

Fig. 14: Solitary waves from Maxwellian condition, *t=12*

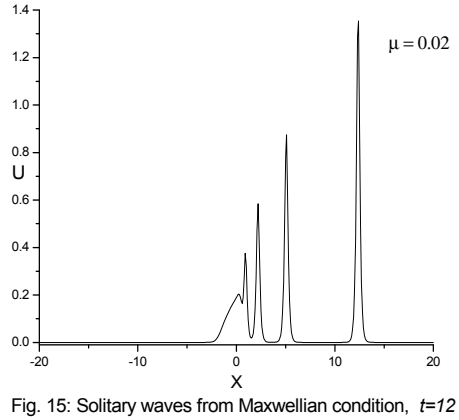

Fig. 15: Solitary waves from Maxwellian condition, *t=12*

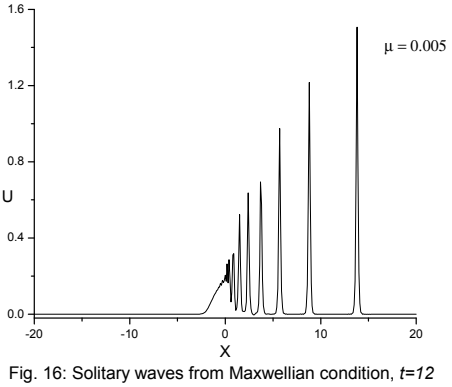

Fig. 16: Solitary waves from Maxwellian condition, *t=12*

the Maxwellian condition does not break into solitons solution but exhibits rapidly oscillating wave packets. When $\mu \approx \mu_c$, a mixed type of solution is obtained which consists of a leading solitons and an oscillating tail. When $\mu << \mu_c$, the Maxwellian condition breaks up in to a number of solitons according to the value of μ. Computations are carried out up to time $t = 12$ with the parameters values $\mu =$ 1, 0.5, 0.1, 0.05, 0.02 and 0.005, $\varepsilon = 3$, $\Delta t = 0.01$, $N = 400$ and the space interval $-20 \leq x \leq 20$ to compare our results with those given in [Evans and Raslan (2005)], [Saka (2007)] and [Zaki (2000)]. For $\mu = 1$ and 0.05, the Maxwellian condition does not generate a clear solitary wave as shown in the Figures 11-12, while for relatively smaller values of $\mu =$ 0.1, 0.05, 0.02 and 0.005 Maxwellian condition breaks down into a number of solitary waves as shown in the Figures 13-16. The invariant quantities C_1, C_2, C_3 corresponding to $\mu =$ 1, 0.5, 0.1 and 0.05 at various times are documented in the Tabs. 6-7 using MQ, GA and TPS. It can be noted from Tabs. 6-7 that the results are in good agreement with those given in [Evans and Raslan (2005)], [Saka (2007)] and [Zaki (2000)]. High accuracy is obtained corresponding to $c =$ 0.4 and 10 for MQ and GA respectively.

Table 6: Invariant quantities for generation of solitary waves from Maxwellian condition

		Our method (MQ)			[Saka (2007)]		
μ	Time	C_1	C_2	C_3	C_1	C_2	C_3
1	0	1.772454	2.506628	0.886227	1.772454	2.506628	0.886227
	6	1.772454	2.506626	0.886227	1.772454	2.506630	0.886227
	12	1.772454	2.506624	0.886227	1.772453	2.506630	0.886227
0.5	0	1.772454	1.879971	0.886227	1.772454	1.879971	0.886227
	6	1.772454	1.879971	0.886227	1.772454	1.879971	0.886227
	12	1.772454	1.879971	0.886227	1.772453	1.879971	0.886227
0.1	0	1.772454	1.378646	0.886227	1.772454	1.378646	0.886227
	6	1.772455	1.378659	0.886250	1.772455	1.378627	0.886264
	12	1.772456	1.378650	0.886261	1.772456	1.378624	0.886265
0.05	0	1.772454	1.315980	0.886227	1.772454	1.315980	0.886227
	6	1.772454	1.315991	0.886417	1.772465	1.315915	0.886452
	12	1.772454	1.315997	0.886432	1.772466	1.315916	0.886454

5 Conclusion

A numerical meshfree technique based on the three different types of RBFs, namely MQ, GA and TPS, has been proposed for the approximate solution of the MEW

Table 7: Invariant quantities for generation of solitary waves from Maxwellian condition

		Our method (GA)			Our method (TPS)		
μ	Time	C_1	C_2	C_3	C_1	C_2	C_3
1	0	1.772454	2.506628	0.886227	1.772454	2.506628	0.886227
	6	1.772454	2.506626	0.886227	1.772453	2.506626	0.886226
	12	1.772453	2.506624	0.886227	1.772452	2.506623	0.886226
0.5	0	1.772454	1.879971	0.886227	1.772454	1.879971	0.886227
	6	1.772454	1.879971	0.886227	1.772454	1.879970	0.886226
	12	1.772454	1.879971	0.886227	1.772454	1.879969	0.886225
0.1	0	1.772454	1.378646	0.886227	1.772454	1.378646	0.886227
	6	1.772455	1.378659	0.886250	1.772455	1.378656	0.886247
	12	1.772456	1.378650	0.886261	1.772455	1.378650	0.886257
0.05	0	1.772454	1.315980	0.886227	1.772454	1.315980	0.886227
	6	1.772454	1.315991	0.886417	1.772504	1.315989	0.886376
	12	1.772454	1.315997	0.886432	1.772503	1.315995	0.886415

equation. The efficiency of the method is tested on the problems of propagation of the single solitary wave, interaction of two solitary waves and development of a train of solitary waves from Maxwellian initial condition. The accuracy is examined in terms of the L_2, L_∞ error norms and the conservation quantities C_1, C_2 and C_3. Stability analysis is performed by the matrix method. The proposed method is simple in applicability and provides high accuracy and invariance of the conserved quantities. The advantage of using TPS is that it is independent of the shape parameter c. The problems presented in this paper suggest that meshfree approximation methods should be considered as one of the possible ways of solving these kinds of nonlinear partial differential equations.

Acknowledgement: The third author is thankful to HEC, Islamabad for financial support under grant # 041-303216/M-112 and Department of Higher Education, Government of NWFP for study leave.

References

Abdulloev, Kh. O.; Bogolubsky, I. L.; Makhankov, V. G. (1976): One more example of inelastic soliton interaction. *Physics Letter*, vol. 56A, pp. 427-428.

Atluri, S. N.; Han, Z. D.; Rajendran, A. M. (2004): A New Implementation of the Meshless Finite Volume Method, Through the MLPG "Mixed" Approach.

CMES: Computer Modeling in Engineering & Sciences, vol. 6(6), pp. 491-514.

Chantasiriwan, S. (2006): Performance of Multiquadric Collocation Method in Solving Lid-driven Cavity Flow Problem with Low Reynolds Number. *CMES: Computer Modeling in Engineering & Sciences*, vol. 15(3), pp. 137-146.

Cheng, A. H. D.; Golberg, M. A.; Kansa, E. J.; Zammito, G. (2003): Exponential convergence and $H-c$ multiquadric collocation method for partial differential equations. *Numer Methods for Partial Diff Eq*, vol. 19, pp. 571-594.

Esen, A. (2006): A lumped Galerkin method for the numerical solution of the modified equal-width wave equation using quadratic B-splines. *Int J Comput Math*, vol. 83(5–6), pp. 449–459.

Esen, A.; Kutluay, S. (2008): Solitary wave solutions of the modified equal width wave equation. *Comm Nonlinear Science and Numer Simul*, vol. 13, pp. 1538–1546.

Evans, D. J.; Raslan, K. R. (2005): Solitary waves for the generalized equal width (GEW) equation. *Int J Comp Math*, vol. 82(4), 445–55.

Fasshauer, G. E. (1996): Solving partial differential equations by collocation with radial basis functions. In: A. L. Me'chaute'(ed.) *Proceedings of Chamonix*, Vanderbilt University Press, Nashville, TN, pp. 1-8.

Franke, C.; Schaback, R. (1998): Solving partial differential equations by collocation with radial basis functions. *Appl Math Comput*, vol. 93, pp. 73-82.

Franke, A.; Schaback, R. (1998): Convergence order estimates of meshless collocation methods using radial basis functions. *Adv Comput Math*, vol. 8, pp. 381–399.

Hamdi, S.; Enright, W. H.; Schiesser, W. E.; Gottlieb J.J. (2003): Exact solutions of the generalized equal width wave equation. *ICCSA*, vol. 2, pp. 725–734.

Hon, Y. C.; Cheung, K. F.; Mao, X. Z.; Kansa, E. J. (1999): Multiquadric solution for shallow water equations. *ASCE J Hydraulic Eng*, vol. 125(5), pp. 524-533.

Hon, Y. C.; Mao, X. Z. (1998): An efficient numerical scheme for Burgers' equation. *Appl Math Comput*, vol. 95(1), pp.37-50.

Hon, Y.C.; Schaback, R. (2001): On unsymmetric collocation by radial basis functions. *Appl Math Comput*, vol. 119 , pp. 177–186.

Kansa, E. J. (1990): Multiquadrics scattered data approximation scheme with applications to Computational fluid-dynamics I, surface approximations and partial derivative estimates. *Comput Math Appl*, vol.19, pp. 127-145.

Khattak, A. J.; Siraj-ul-Islam (2008): A comparative numerical solutions of a class of KdV equations. *Appl Math Comput*, vol. 199, pp. 425–434.

Kosec, G.; Sarler, B. (2008): Local Collocation Method for Darcy Flow. *CMES: Computer Modeling in Engineering & Sciences*, vol. 25(3), pp. 197-207.

Li, J.; Chen, Y.; Pepper, D. (2003): Radial basis function method for 1-D and 2-D groundwater contaminant transport modeling. *Comput Mech*, vol. 32, pp. 10–15.

Lorentz, R. A.; Narcowich, F. J.; Ward, J. D. (2003): Collocation discretizations of the transport equation with radial basis functions. *Appl Math Comput*, vol.145, pp. 97–116.

Lu, J. (2007): He's variational iteration method for the modified equal width equation. *Chaos, Solitons and Fractals*, In press.

Morrison, P. J.; Meiss, J. D.; Carey, J. R. (1984): Scattering of RLW solitary waves. *Physica D*, vol. 11, pp. 324–336.

Peregrine, A. H. (1966): Calculations of the development of an undular bore. *J Fluid Mech*, vol. 25(2), pp. 321-330.

Rubin, S. G.; Graves, R. A. (1975): Cubic spline approximation for problems in fluid mechanics. *NASA TR* R-436, Washington, DC.

Saka, B. (2007): Algorithms for numerical solution of the modified equal width wave equation using collocation method. *Math Comp Modl*, vol. 45, pp. 1096–1117.

Siraj-ul-Islam; Sirajul Haq; Arshed Ali (2008): A meshfree method for the numerical solution of RLW equation, *J. Comp. Appl. Math*, DOI: 10.1016.

Siraj-ul-Islam; Sirajul Haq; Marjan Uddin (2008): A meshfree interpolation method for the numerical solution of the coupled nonlinear partial differential equations. *Eng Anal Bound Elem*, In Press.

Wazwaz, A. M. (2006): The tanh and sine–cosine methods for a reliable treatment of the modified equal width equation and its variants. *Comm Nonlinear Sci Numer Simul*, vol. 11, pp. 148–160.

Wu, Z.; Hon, Y. C. (2003): Convergence error estimates in solving free boundary diffusion problem by radial basis functions method. *Eng Anal Bound Elem*, vol. 27, pp. 73–79.

Zaki, S. I. (2000): Solitary wave interactions for the modified equal width equation. *Comput Phys Comm*, vol.126, pp. 219–231.